Investigation of the effect of using various HFC refrigerants in geothermal heat pump with residential heating applications

Mahdi Deymi-Dashtebayaz[1] · Saeed Maddah[1] · Marjan Goodarzi[2] · Omid Maddah[3]

Abstract

In the present investigation, the impact of various refrigerants on the efficiency of the geothermal heat pump operation is investigated. Appropriate working range of five HFC refrigerants such as R125, R134A, R404A, R407C, and R507A for using a geothermal heat pump is studied. Also, the energy and exergy analysis is used to investigate the influence of varying temperatures of the exhaust fluid from the geothermal source on heat pump operation. The critical parameters, such as coefficient of performance (COP), exergy efficiency, and exergy destruction for various components, are calculated. The results show that, in the geothermal heat pump cycle, R134A and R125 refrigerants have the highest and lowest COP and exergy efficiency, respectively. Moreover, enhancing the temperature of the exhaust fluid from the geothermal source results in an enhancement of the COP. For the mentioned refrigerants, the exergy destruction due to the compressor, as the primary energy-consuming equipment, is obtained between 26.7 and 27.3% range relative due to the overall system. The outcomes achieved in present research may provide the instructions for the design and optimization of efficient geothermal heat pump systems.

List of symbols

$\dot{E}$	Energy ratio (kW)
$\dot{Ex}$	Exergy ratio (kW)
h	Enthalpy (kJ kg^{-1})
$\dot{m}$	Mass flow rate (kg s^{-1})
P	Pressure (kPa)
$\dot{Q}$	Heat transfer (kW)
s	Specific entropy (kJ kg^{-1} K^{-1})
T	Temperature (K)
$\dot{W}$	Power consumption (kW)

Greek symbols

Δ	Differences
η	Efficiency
ψ	Exergy change for per mass at open system (kW)

Subscripts

1–13	State points in Fig. 1
0	Ambient
a	Each system part
AT	Accumulation tank
Comp	Compressor
Cond	Condenser
dest	Destruction
Eva	Evaporator
G	Underground heat exchanger
in	Inlet
P	Output panels
P1	Pump 1
P2	Pump 2
P3	Pump 3
out	Outlet

Abbreviations

COP	Coefficient of performance
GWP	Global warming potential

✉ Marjan Goodarzi
marjan.goodarzi@tdtu.edu.vn

1 Center of Computational Energy, Department of Mechanical Engineering, Hakim Sabzevari University, Sabzevar, Iran

2 Sustainable Management of Natural Resources and Environment Research Group, Faculty of Environment and Labour Safety, Ton Duc Thang University, Ho Chi Minh City, Vietnam

3 Toklan Toos Industry Co., Mashhad, Iran

HFC   Hydrofluorocarbons
ODP   Ozone depletion potential

Introduction

As the world's population grows fast, and the pattern of life changes, the consumption of fossil fuels gradually increases. Using fossil fuels causes some problems, including environmental pollution and depletion of limited resources [1, 2]. Therefore, renewable resources such as geothermal energy are already expanding, because they are environment friendly as well as spontaneously refresh in a natural process.

The heat pumps are technologies that can use renewable sources and utilize the thermal energy of various sources at relatively high temperatures to be used in the process of air conditioning for different sectors. Because heat pumps could work with low-temperature energy sources such as solar energy, waste heat from industries, and low-temperature geothermal energy, these energies could be used in the heat pump cycle. Recently, the examination of the heat pump with a relatively low-temperature source focused on the choice of suitable operating fluid based on the typical temperature of the heat pump cycle equipment [3–10]. The energy analysis is employed to evaluate the use of low-temperature source

in heat pumps. It is found that the coefficient of performance (COP) of the geothermal heat pump is higher than the air-source heat pump [11]. In another study, Lee et al. [12] determined the location of the optimum borehole of the geothermal heat pump. Their results show that smaller borehole separation and higher groundwater flow cause thermal efficiency improvement.

Refrigerants play a vital role in the heat pump performance regarding the thermodynamic properties. Some properties such as compatibility, safety, stability, availability of refrigerant, cost, and environmental influences are attention for these systems. Common refrigerants used in the heat pump cycles are usually between the two primary refrigerants of the halocarbons and hydrocarbons. Due to the environmental effects, using some refrigerants, especially chlorofluorocarbons (CFCs) and hydrochlorofluorocarbons (HCFCs), is limited for their use. The Montreal Protocol to protect the environment seriously emphasizes the issue of reducing the consumption and production of CFCs and HCFCs. [13]. Some articles [14–17] carried out experimental researches on many pure and mixtures of fluorinated fluids. Wang [18] studied the usage outlook of natural working fluids in China. Also, based on these studies, the development of the compressor in the heat pump system is studied. Hydrocarbons are also considered to be fine CFCs substitutes [19]. Some investigations [20–22]

Fig. 1 Schematic of a geothermal heat pump in heating process
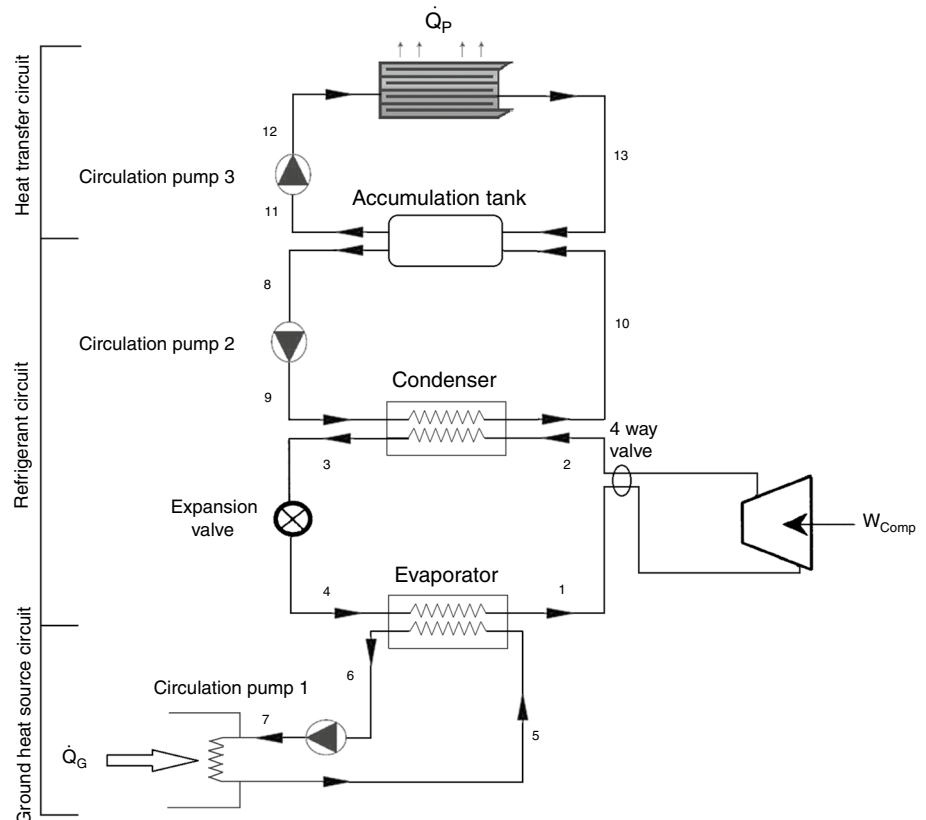
conducted on the compression refrigeration cycle with working fluid. They explored that the essential parameters can be controlled by changing the speed of compressor rotation. Some hydrocarbons have high cycle performance, but their use is limited due to their explosiveness.

Many refrigerants in HFCs group, such as R125, R134a, R404A, R407C, R410A, R422A, R422B, R422C, R422D, and R507A, are good choices to replace CFCs, because they neither contain chlorine and bromine nor deplete the ozone layer (ODP = 0) [23]. Based on this, various studies performed energy analysis to replace hydrochlorofluorocarbons (HCFC) as R22 refrigerant [24–31]; however, exergy analysis is instrumental in improving the engineering systems [32, 33].

The heat pump cycle saves energy and is very efficient in recycling heat. However, when these systems are used to supply heat under conditions such as high-temperature supply and the high-pressure ratio between condensation pressure and evaporation pressure, the efficiency of these cycles is reduced. Therefore, many studies have been done to prevent COP depletion in heat pump systems [34–42]. Also, in these systems, the high-temperature difference between the supply water and the operating fluid in the condenser causes plenty of irreversible losses in the heat transfer process. Many kinds of research are performed to increase the performance of high-temperature heat pumps [43–47].

In the present research, a simulation of a geothermal heat pump sample is performed. In addition to the use of various HFC refrigerants' impact on the performance cycle, the effect of different temperatures of the exhaust fluid from the geothermal source is investigated. Also, the impact of changes in the isentropic efficiency of the compressor in the COP and exergy efficiency of the geothermal heat pump cycle is carried out. A thermodynamic model based on mass, energy, and exergy balance is developed to calculate the variation in the COP, exergy efficiency, and exergy destruction for geothermal heat pump cycle equipment. The analysis is done to improve the coefficient of operation of the geothermal heat pump cycle and select the best refrigerant according to those five refrigerant operating conditions.

Configuration of a geothermal heat pump cycle

In Fig. 1, the schematic of a geothermal heat pump is observed in the heating process. This cycle includes three primary parts: the ground heat source circuit, the refrigerant circuit, and the output heat circuit. The main components of this cycle are geothermal exchangers, evaporators, compressors, condensers, expansion valves, accumulation tank, output heat panels, and three pumps. A 500-L storage tank is used in this cycle, which is insulated to prevent heat losses. This accumulation tank is consistently providing the required heating load. Heat output panels are considered as a heat exchanger that has the duty of distributing energy in the building. In the ground heat circuit, the heat is transmitted between the soil and the geothermal exchangers ($\dot{Q}_G$). The output fluid of accumulation tank is transferred to various places through the output panels ($\dot{Q}_P$). The studied case is proposed to use in a residential building with a 5.7 kW heat load.

Some characteristics of HFC refrigerants used in this study are given in Table 1. As evident, different groups of HFCs, including pure refrigerants (R125 and R134A), zeotropic mixtures (R404A and R407C), and azeotropic mixtures (R507A), are selected.

As shown, although some HFCs have high GWPs due to the higher COP factor and lower CO_2 emissions caused by energy consumption, the use of these refrigerants is common in the heat pumps. Besides, in many places around the world, recycling and reclamation of these refrigerants are counseled to decrease its direct global warming influence [23].

Thermodynamic model

Some assumptions are made for thermodynamic analysis of the heat pump system as follows:

- The investigated system is in steady-state conditions.
- The compressor isentropic efficiency is constant, and the compression process in compressors is considered as adiabatic.

Table 1 Some characteristics of HFC refrigerants

Type	Fluid	GWP$_{100 \text{ years}}$ /kg$_{eq}$CO$_2$kg^{-1}	ODP	Critical temp./°C	Critical pressure (absolute)/kPa	Atmospheric lifetime/years
HFC	R125	3500	0	66.18	3629	29
HFC	R134A	1430	0	101.06	4059	14
HFC	R404A	3922	0	72.14	3735	40.36
HFC	R407C	1774	0	86.05	4634	15.657
HFC	R507A	3985	0	70.74	3715	40.5

- The throttling processes in throttling valves are considered as isenthalpic.
- The pressure drop and heat loss of refrigerant in the cycle are neglected, and heat transfer processes in evaporator and condenser are constant pressure process.
- The kinetic and potential energy variations are neglected.

The thermodynamic model is obtained according to the conservation principle of mass, energy, and exergy of the main components of the heat pump cycle.

The detailed formulations about energy analysis of the case study with the mentioned assumptions are presented as Eqs. (1), (2), and (3):

$$\dot{E}_{in} - \dot{E}_{out} = \Delta\dot{E}_{system} \tag{1}$$

$$\dot{m}_{in}h_{in} = \dot{m}_{out}h_{out} \tag{2}$$

$$\dot{Q}_{in} + \dot{W}_{in} + \dot{m}_{in}h_{in} = \dot{Q}_{out} + \dot{W}_{out} + \dot{m}_{out}h_{out} \tag{3}$$

In Eqs. (4), (5) and (6), $(\dot{Q}_G)$ and $(\dot{Q}_P)$ indicate the heat transfer to the underground heat exchanger and the required heating load, respectively. Also, $(\dot{W}_{comp})$ and $(\dot{W}_p)$ are consuming work of the compressor and pumps, respectively.

For all heating processes based on Fig. 1, energy conservation is written as below:

$$\dot{E}_{in} = \dot{Q}_G + \dot{W}_{comp} + \dot{W}_{P1} + \dot{W}_{P2} + \dot{W}_{P3} \tag{4}$$

$$\dot{E}_{out} = \dot{Q}_P + \dot{Q}_{loss} \tag{5}$$

$$\dot{Q}_P + \dot{Q}_{loss} = \dot{Q}_G + \dot{W}_{comp} + \dot{W}_{P1} + \dot{W}_{P2} + \dot{W}_{P3} \tag{6}$$

The coefficient of efficiency of the system in the heating process based on Fig. 1 is calculated by Eq. (7).

$$COP_{heating} = \frac{\dot{Q}_P}{\dot{W}_{comp} + \dot{W}_{P1} + \dot{W}_{P2} + \dot{W}_{P3}} \tag{7}$$

Exergy is the maximum useful work that can be obtained from the energy. Exergy analysis is a method that evaluates the thermodynamic performance of different systems based on the second law of thermodynamics. The equation of exergy balance can be defined as Eq. (8).

$$\dot{Ex}_{in} - \dot{Ex}_{out} = \dot{Ex}_{dest} \tag{8}$$

Therefore, using Eq. (9), the exergy balance in general mode is introduced as Eq. (10).

$$\psi = (h - h_0) - T_0(s - s_0) \tag{9}$$

$$\dot{Q}_a\left(1 - \frac{T_0}{T_a}\right) - \dot{W} + \dot{m}_{in}\psi_{in} - \dot{m}_{out}\psi_{out} = \dot{Ex}_{dest} \tag{10}$$

where $\dot{W}$ is the work rate and $\dot{Q}_a$ is the heat transfer rate at temperature T_a at the location a. The reference temperature of the environment is (T_0) and the exergy destruction is $(\dot{Ex}_{dest})$.

Specific exergy in an open system (ψ) of a flowing fluid is illustrated as follows:

For the analyzed system, general exergy balance based on Fig. 1 is defined by Eq. (11):

$$\dot{Q}_G\left(1 - \frac{T_0}{T_G}\right) + \dot{W}_{comp} + \dot{W}_{P1} + \dot{W}_{P2} + \dot{W}_{P3} - \dot{Q}_P\left(1 - \frac{T_0}{T_P}\right) = \dot{Ex}_{dest} \tag{11}$$

For general examples that do not produce or consume work, the exergy efficiency is expressed as Eq. (12) [23]:

$$\eta_{Exergy} = \frac{\text{Exergy recovered}}{\text{Exergy supplied}} \tag{12}$$

The exergy efficiency for this system based on Fig. 1 is expressed by Eq. (13):

$$\eta_{Exergy} = \frac{\dot{Q}_P\left(1 - \frac{T_0}{T_P}\right)}{\dot{W}_{comp} + \dot{W}_{P1} + \dot{W}_{P2} + \dot{W}_{P3} + \dot{Q}_G\left(1 - \frac{T_0}{T_G}\right)} \tag{13}$$

For the thermodynamic analysis, the equations illustrated in Table 2 are used for the equipment of the investigated cycle in the heating process based on Fig. 1.

Model validation

To validate the mathematical method in this study, the results of the numerical method are compared with available experimental results [48]. The specifications of the input variables for validation are presented in Table 3. Also, the COP of the heat pump is computed for R410A refrigerant in comparison with the experimental data found in Ref. [48]. The COP obtained from the experimental data is 4.23, and, with our calculation, it is 4.07. The relative errors between the experimental outcomes and our simulations are about 3.93%. Also, the experimental temperature of different points of Ref. [48] cycle and COP and energy consumption of the compressor is compared with the calculation program and presented in Tables 4 and 5. As shown in this table, there is good accordance between the numerical and experimental results.

Table 2 Energy and exergy balance of equipment in the heating process

Equipment	Energy balance	Exergy balance
Compressor	$\dot{E}_1 + \dot{W}_{\text{Comp}} = \dot{E}_2 + \dot{Q}_{\text{loss.Comp}}$	$\dot{Ex}_1 + \dot{W}_{\text{Comp}} = \dot{Ex}_2 + \dot{Ex}_{\text{dest.Comp}}$
Condenser	$\dot{E}_2 + \dot{E}_9 = \dot{E}_3 + \dot{E}_{10} + \dot{Q}_{\text{loss.Cond}}$	$\dot{Ex}_2 + \dot{Ex}_9 = \dot{Ex}_3 + \dot{Ex}_{10} + \dot{Ex}_{\text{dest.Cond}}$
Evaporator	$\dot{E}_4 + \dot{E}_5 = \dot{E}_1 + \dot{E}_6 + \dot{Q}_{\text{loss.Eva}}$	$\dot{Ex}_4 + \dot{Ex}_5 = \dot{Ex}_1 + \dot{Ex}_6 + \dot{Ex}_{\text{dest.Eva}}$
Expansion valve	$\dot{E}_3 = \dot{E}_4$	$\dot{Ex}_3 = \dot{Ex}_4 + \dot{Ex}_{\text{loss.valve}}$
Pump 1	$\dot{E}_6 + \dot{W}_{\text{P1}} = \dot{E}_7 + \dot{E}_{\text{loss.P1}}$	$\dot{Ex}_6 + \dot{W}_{\text{P1}} = \dot{Ex}_7 + \dot{Ex}_{\text{dest.P1}}$
Pump 2	$\dot{E}_8 + \dot{W}_{\text{P2}} = \dot{E}_9 + \dot{E}_{\text{loss.P2}}$	$\dot{Ex}_8 + \dot{W}_{\text{P2}} = \dot{Ex}_9 + \dot{Ex}_{\text{dest.P2}}$
Pump 3	$\dot{E}_{11} + \dot{W}_{\text{P3}} = \dot{E}_{12} + \dot{E}_{\text{loss.P3}}$	$\dot{Ex}_{11} + \dot{W}_{\text{P3}} = \dot{Ex}_{12} + \dot{Ex}_{\text{dest.P3}}$
Underground heat exchanger	$\dot{Q}_{\text{G}} + \dot{E}_7 = \dot{E}_5 + \dot{Q}_{\text{loss.G}}$	$\dot{Ex}_{\text{G}} + \dot{Ex}_7 = \dot{Ex}_5 + \dot{Ex}_{\text{dest.G}}$
Accumulation tank	$\dot{E}_{10} + \dot{E}_{13} = \dot{E}_8 + \dot{E}_{11} + \dot{Q}_{\text{loss.AT}}$	$\dot{Ex}_{10} + \dot{Ex}_{13} = \dot{Ex}_8 + \dot{Ex}_{11} + \dot{Ex}_{\text{dest.AT}}$
Output panels	$\dot{E}_{12} = \dot{E}_{13} + \dot{Q}_{\text{P}} + \dot{Q}_{\text{loss.P}}$	$\dot{Ex}_{12} = \dot{Ex}_{13} + \dot{Ex}_{\text{P}} + \dot{Ex}_{\text{dest.P}}$

Table 3 Specifications of the cycle in Ref. [48]

Name of the measured parameter	Nominal value	Unit
Condenser outlet temperature (gas)	28.37	°C
Evaporator inlet temperature (gas)	− 0.14	°C
Mass flow rate (R410A)	0.035	kg s^{-1}
Heating capacity	6.7	kW

Table 4 Some comparison of temperature points of the cycle of calculation program with Ref. [48]

Flow number	Present study T/K	Ref. [48] T/K	Error/%
1	288.6	281.12	2.66
2	344.6	336.31	2.46
3	305.8	301.52	1.42
4	273	273.01	0.04
5	280.6	280.63	0.01
6	277	277.04	0.01
7	277	277.09	0.03
8	302.8	302.8	0
9	302.9	302.85	0.02
10	305.9	305.81	0.03
11	303.7	303.75	0.02
12	303.7	303.85	0.05
13	297.9	297.92	0.007

Table 5 Comparison of COP and energy consumption of the compressor with Ref. [48]

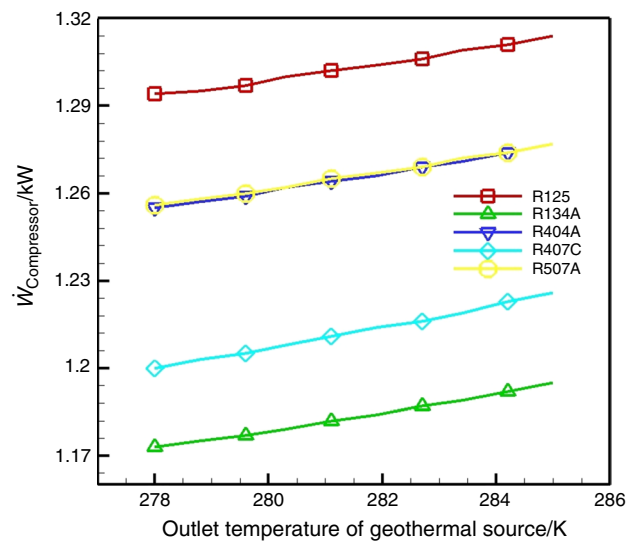| Parameter	Present study	Ref. [48]	Error/%
COP	4.07	4.24	4.01
Power consumption of compressor (kW)	1.33	1.27	4.72

Fig. 2 Change of the compressor work for various refrigerants with the outlet temperature of the geothermal source

Results and discussions

In this investigation, the heat pump is studied concerning the cooling capacity of 5.7 kW with condenser temperature of 303.15 K and evaporator temperature of 272.15 K. Based on this, the influence of different HFC refrigerants is investigated on the performance of the geothermal heat pump. The first and second laws of thermodynamic equations are solved to study the effect of varying temperature of the exhaust fluid from the geothermal source on the geothermal heat pump operation.

According to Fig. 2, the work of compressor with the temperature of the exhaust fluid from the geothermal source for R125, R134A, R404A, R407C, and R507A refrigerants is plotted. As shown in Fig. 2, R125 refrigerant has a higher function of the compressor. Also, R134A

and R407C refrigerants have lower compressor work, respectively. R507A and R404A refrigerants also have moderate compressor work. It is also observed that, with the increment of the temperature of the exhaust fluid from the geothermal source, the compressor work is accordingly augmented. The rate of change in the compressor work with the temperature of the exhaust fluid from the geothermal source is higher for R407C, R134A, R404A, R507A, and R125 refrigerants, respectively.
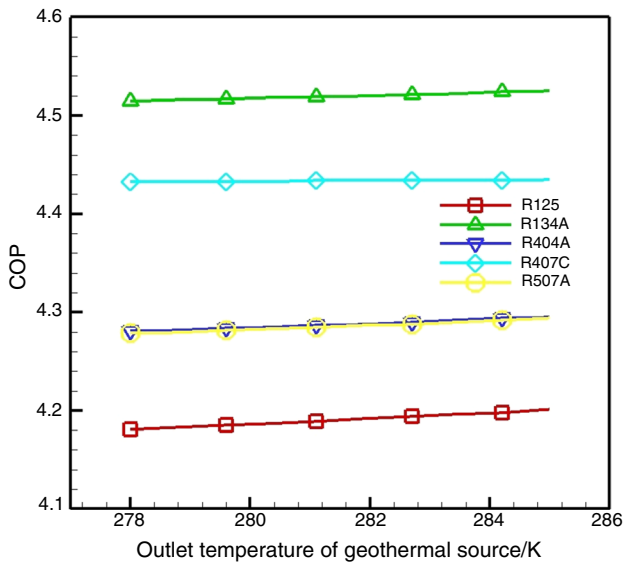
According to Fig. 3, the heat pump cycles using R4134A and R125 refrigerants have the highest and lowest COP among the compared refrigerants based on Eq. (7). Due to
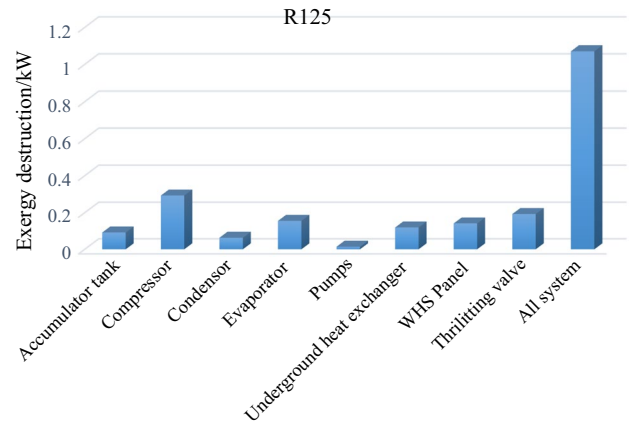
(a) Exergy destruction due to the equipment in the studied cycle with R125 refrigerant.

Fig. 3 Change of COP for various refrigerants with the outlet temperature of the geothermal source
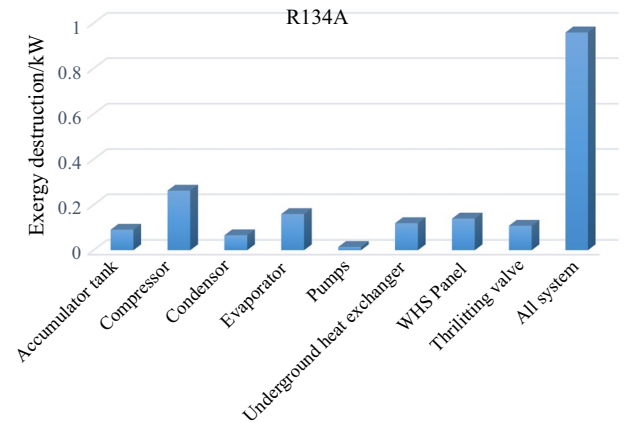
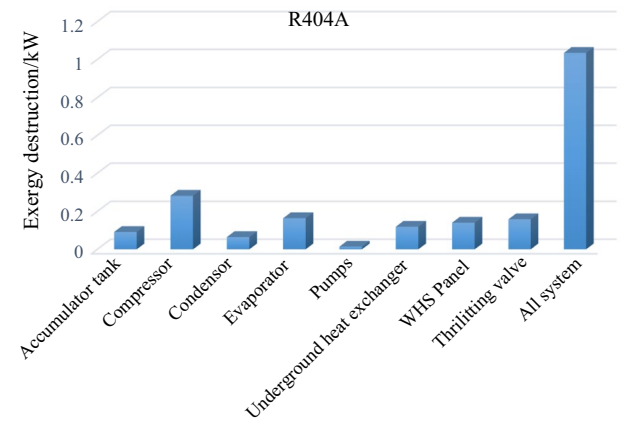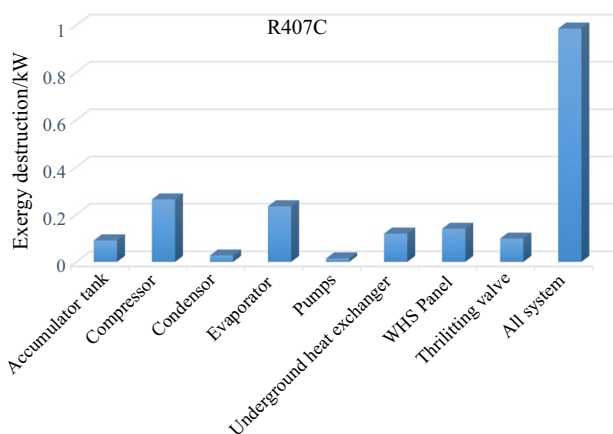**(b)** Exergy destruction due to the equipment in the studied cycle with R134A refrigerant.

Fig. 4 Change of COP for different refrigerants with isentropic efficiency of the compressor
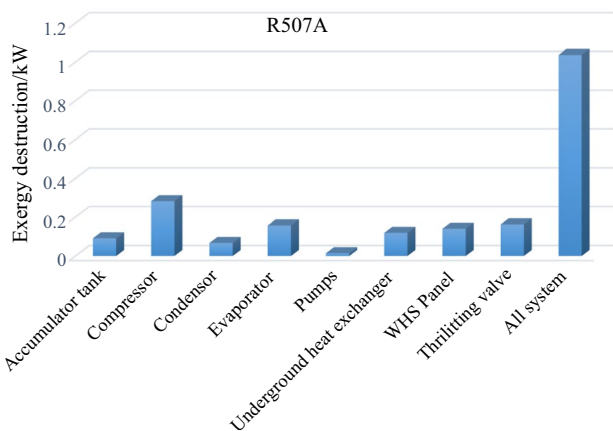
(c) Exergy destruction due to the equipment in the studied cycle with R404A refrigerant.

Fig. 5 Comparison of exergy destruction due to the equipment in the studied cycle for different refrigerants

(d) Exergy destruction due to the equipment in the studied cycle with R407C refrigerant.

(e) Exergy destruction due to the equipment in the studied cycle with R507A refrigerant.

Fig. 5 (continued)

the increasing temperature of exhaust fluid from the geothermal source, the heat output from the panel increases more than the work of the compressor, thus expanding the COP. Also, as illustrated, increasing the temperature of exhaust fluid from the geothermal source enhances the COP of the cycle for all the refrigerants. Increasing the temperature of the exhaust fluid from the geothermal source for R125, R507A, and R404A, respectively, is more effective than the other refrigerants, and the slope of COP of these refrigerants is higher. R407C and R134A refrigerants show the slightest variation with an enhancement in the exhaust fluid temperature from the geothermal source.

As shown in Fig. 4, the impact of changes on the isentropic efficiency of the compressor on the COP is investigated. It is observed that the isentropic efficiency of the compressor has a direct effect on all the refrigerants. Increasing isentropic efficiency reduces the work of the compressor and enhances the COP based on Eq. 7. The enhancement

of the COP is not the same as different refrigerants with an isentropic efficiency of the compressor, and R125 and R507A refrigerants have the lowest variations, respectively; R134A and R407C refrigerants, respectively, have the most significant changes in terms of this parameter.

In Fig. 5, the exergy destruction of the heat pump equipment is plotted for different HFC refrigerants. Based on Eq. (10), R125 and R134A have the highest and lowest exergy destruction in the heat pump cycle. On the other hand, among the heat pump equipment, the compressor has the most top exergy destruction. Also, R125 refrigerant has
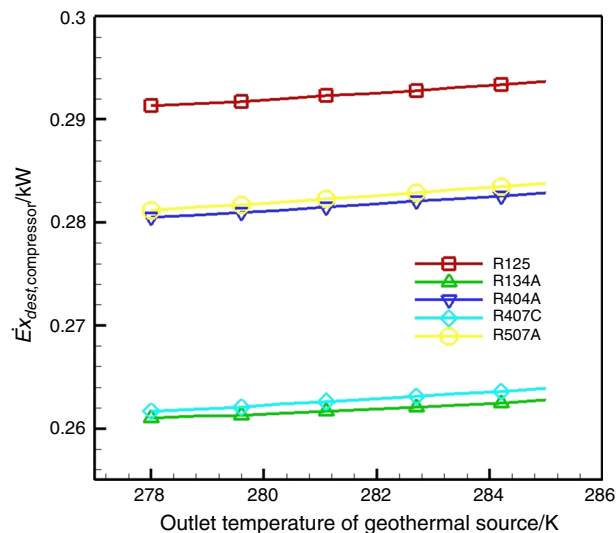

Fig. 6 Comparison of exergy destruction due to the compressor for different refrigerants with the outlet temperature of the geothermal source
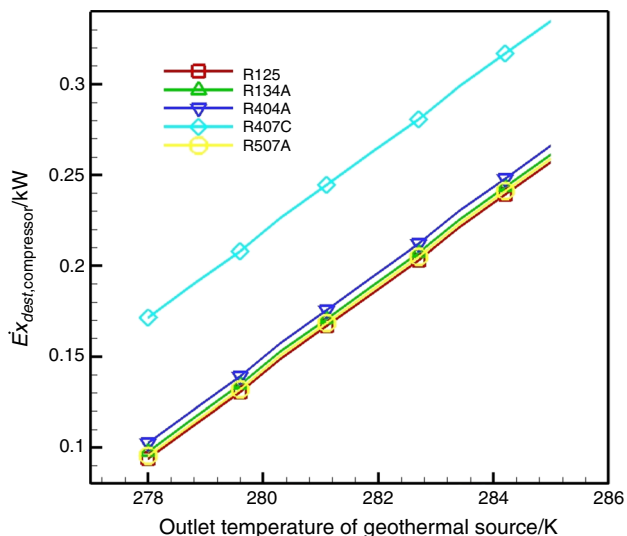

Fig. 7 Comparison of exergy destruction due to the evaporator for different refrigerants with the outlet temperature of the geothermal source
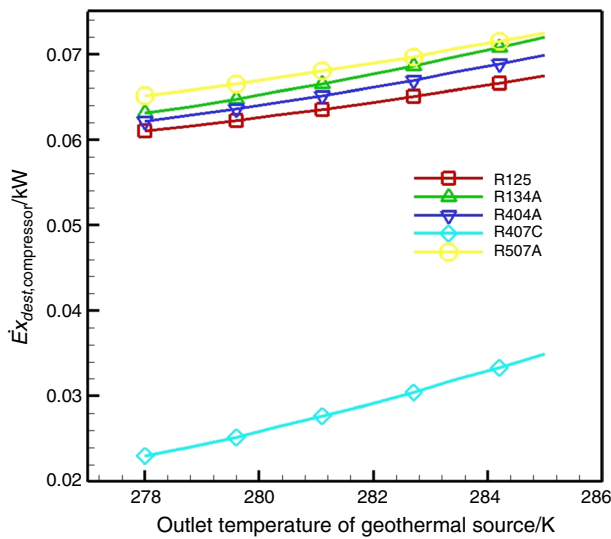
Fig. 8 Comparison of exergy destruction due to the condenser for different refrigerants with the outlet temperature of geothermal source
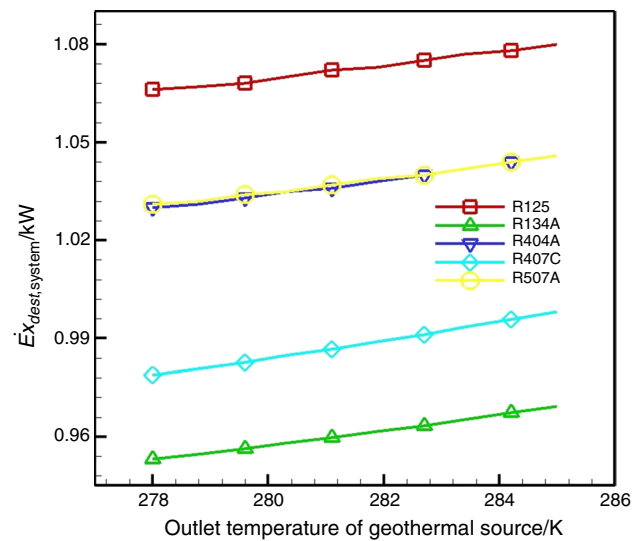

Fig. 10 Comparison of exergy destruction due to the whole system for different refrigerants with the outlet temperature of the geothermal source

the highest exergy destruction due to the compressor, and its value is 0.2921 kW.

In Fig. 6, the exergy destruction due to the compressor with the temperature of the exhaust fluid from the geothermal source is observed for various refrigerants. R125 refrigerant has the most exergy destruction due to the compressor, and, in contrast to R134A, the exergy destruction due to the compressor is approximately equal to the smallest amount of this parameter among the comparative refrigerants in the heat pump cycle. R134A refrigerants have the least exergy

destruction due to the compressor changes with the temperature of the exhaust fluid from the geothermal source.

The exergy destruction due to the evaporator with the temperature of the exhaust fluid from the geothermal source for various refrigerants is presented in Fig. 7. R407C refrigerant has the most exergy destruction due to the evaporator among the comparable refrigerants in the heat pump cycle. R507A refrigerant has the highest variations of exergy destruction of the evaporator with the temperature of the exhaust fluid from the geothermal source, among other
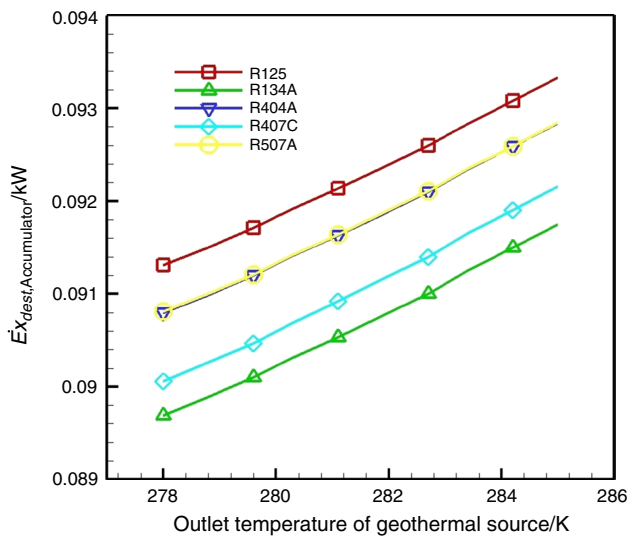

Fig. 9 Comparison of exergy destruction due to the accumulator tank for different refrigerants with the outlet temperature of the geothermal source
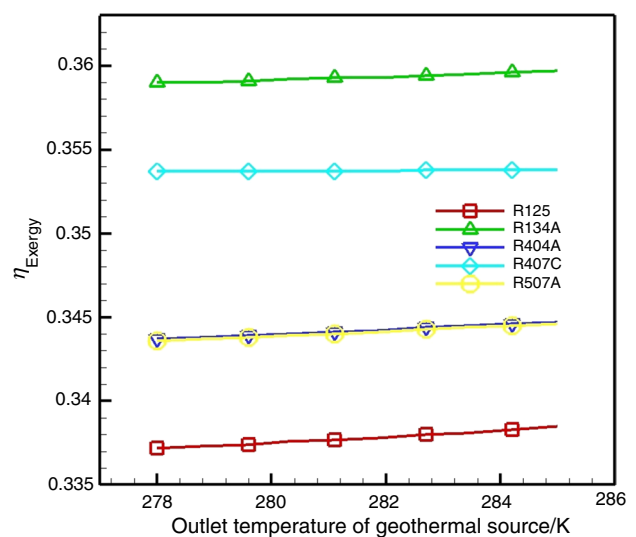

Fig. 11 Comparison of exergy efficiency for different refrigerants with the outlet temperature of the geothermal source
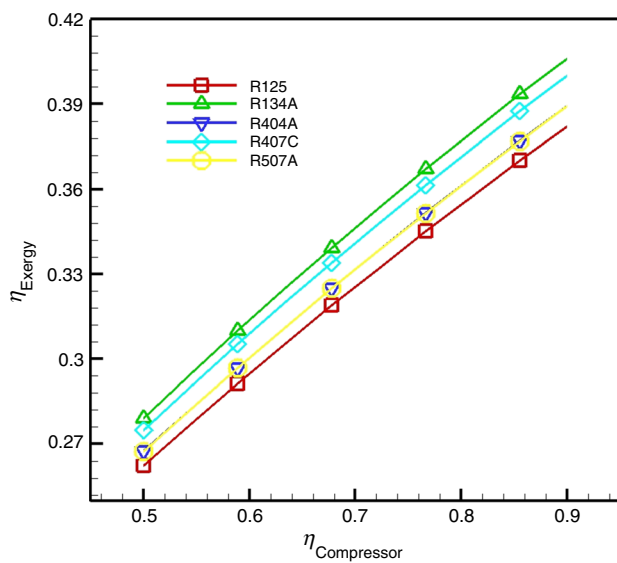
Fig. 12 Comparison of exergy efficiency for different refrigerants with isentropic efficiency of the compressor

refrigerants. The changes of exergy destruction due to the evaporator decrease for R404A, R125, R134A, and R407C, respectively. The variation in the temperature of the exhaust fluid from the geothermal source has a direct impact on the evaporator equipment, so according to Eq. 10, exergy destruction has a very steep slope for all refrigerants due to the increased heat exchange rate in this equipment.

According to Fig. 8, the exergy destruction due to the condenser with the temperature of the exhaust fluid from the geothermal source for various refrigerants is compared. R507A refrigerant has the highest amount of exergy destruction due to the condenser. The exergy destruction reduces due to the condenser for R134A, R404A, R125, and R407C refrigerants, respectively. Also, R407C refrigerant has the highest variations of exergy destruction due to the condenser with the temperature of the exhaust fluid from the geothermal source, among other refrigerants. The change of exergy destruction of the condenser decreases for R134A, R404A, R507A, and R125, respectively.

According to Fig. 9, the exergy destruction due to the accumulator tank with the temperature of the exhaust fluid from the geothermal source for the various refrigerants shows that R125 refrigerant has the highest exergy destruction due to the accumulation tank, and, then, the exergy destruction reduces due to the accumulator tank for R507A, R404A, R407C, and R134A, respectively. The change of the exergy destruction due to the accumulator tank with the temperature of the exhaust fluid from the geothermal source is approximately equal for the various refrigerants.

In Fig. 10, the exergy destruction due to the whole system is compared with the temperature of the exhaust fluid from the geothermal source for various refrigerants, according to (11). Due to the parameters in this equation and the higher exergy of the heat input to the cycle and the cycle work consumed than the exergy of the heat output from the cycle, the total system exergy destruction is increased. R125

Table 6 Major thermodynamics properties data and exergy rates for geothermal heat pump with different refrigerants in the heating process. State numbers refer to Fig. 1

Refrigerant	Flow number	$\dot{m}$/kg s^{-1}	P/kPa	T/K	h/kJ kg^{-1}	s/kJ kg^{-1} K^{-1}	$\dot{Ex}$/kW
R125	1	0.0656	650	280.9	340.3	1.515	2.164
	2	0.0656	1568	317.4	360.1	1.531	3.173
	3	0.0656	1568	303.1	239.9	1.136	2.373
	4	0.0656	650	272.2	239.9	1.147	2.181
R134A	1	0.0401	282	280.9	257.6	0.9602	0.8706
	2	0.0401	770	323	287.1	0.9841	1.789
	3	0.0401	770	303.1	93.54	0.3477	0.9987
	4	0.0401	282	272.1	93.54	0.3576	0.8909
R404A	1	0.0504	581	280.8	373.8	1.639	1.918
	2	0.0504	1414	320.3	398.8	1.659	2.9
	3	0.0504	1414	302.8	243.2	1.148	2.102
	4	0.0504	581	271.7	243.2	1.159	1.944
R407C	1	0.0362	445	281.6	417.8	1.809	1.34
	2	0.0362	1176	330	451.2	1.836	2.286
	3	0.0362	1176	297.7	236	1.124	1.532
	4	0.0362	445	267.2	236	1.134	1.434
R507A	1	0.0521	605	280.4	369.6	1.623	2.164
	2	0.0521	1459	319.5	393.9	1.643	3.173
	3	0.0521	1459	303.1	243.3	1.148	2.373
	4	0.0521	605	272.2	243.3	1.159	2.181

Table 7 Exergy destruction for geothermal heat pump equipment with (a) R125 refrigerant in heating process, (b) R134A refrigerant in heating process, (c) R404A refrigerant in heating process, (d) R407C refrigerant in heating process, (e) R507A refrigerant in heating process

Control volume	$\dot{E}x_{in}$/kW	$\dot{E}x_{out}$/kW	$\dot{E}x_{dest}$/kW	η_{Exergy}/%
(a)				
Compressor	3.464	3.173	0.291	91.6
Evaporator	2.435	2.278	0.157	93.5
Throttling valve	2.373	2.181	0.192	91.9
Condenser	6.877	6.813	0.064	99.1
Underground heat exchanger	0.373	0.254	0.119	68.1
Accumulator tank	5.612	5.52	0.092	98.4
Output panels	1.859	1.718	0.141	92.4
All system	1.616	0.546	1.07	33.8
(b)				
Compressor	2.051	1.789	0.262	87.2
Evaporator	1.145	0.985	0.16	86
Throttling valve	0.999	0.891	0.108	89.2
Condenser	5.493	5.427	0.066	98.8
Underground heat exchanger	0.373	0.254	0.119	68.1
Accumulator tank	5.6	5.51	0.09	98.4
Output panels	1.849	1.709	0.14	92.4
All system	1.496	0.537	0.959	35.9
(c)				
Compressor	3.18	2.9	0.28	91.2
Evaporator	2.198	2.032	0.166	92.4
Throttling valve	2.102	1.944	0.158	92.5
Condenser	6.604	6.538	0.066	99
Underground heat exchanger	0.373	0.254	0.119	68.1
Accumulator tank	5.608	5.517	0.091	98.4
Output panels	1.856	1.715	0.141	92.4
All system	1.578	0.543	1.035	34.4
(d)				
Compressor	2.549	2.286	0.263	0.9
Evaporator	1.688	1.454	0.234	86.1
Throttling valve	1.532	1.434	0.098	93.6
Condenser	5.99	5.963	0.027	99.5
Underground heat exchanger	0.373	0.254	0.119	68.1
Accumulator tank	5.603	5.512	0.091	98.4
Output panels	1.851	1.711	0.14	92.4
All system	1.525	0.539	0.986	35.3
(e)				
Compressor	3.264	2.982	0.282	91.4
Evaporator	2.273	2.115	0.158	93
Throttling valve	2.182	2.019	0.163	92.5
Condenser	6.686	6.618	0.068	99
Underground heat exchanger	0.373	0.254	0.119	68.1

Table 7 (continued)

Control volume	$\dot{E}x_{in}$/kW	$\dot{E}x_{out}$/kW	$\dot{E}x_{dest}$/kW	η_{Exergy}/%
Accumulator tank	5.608	5.517	0.091	98.4
Output panels	1.856	1.715	0.141	92.4
All system	1.579	0.543	1.036	34.4

Table 8 Percent of exergy destruction due to the compressor of the geothermal heat pump for various refrigerants

Refrigerant	R125	R134A	R404A	R407C	R507A
Percent of exergy destruction	27.2	27.3	27	26.7	27.2

refrigerant has the highest exergy destruction, and, after that, the exergy destruction of the system has decreased for R507A, R404A, R407C, and R134A refrigerants, respectively. Also, the most significant changes are observed in the exergy destruction due to the whole system with the temperature of the exhaust fluid from the geothermal source for R407C refrigerant and the least variation for R125 coolant.

According to Fig. 11, the exergy efficiency calculated by Eq. (13) is shown with the temperature of the exhaust fluid from the geothermal source for various refrigerants. R134A refrigerant has the highest exergy efficiency, and, then, the exergy efficiency decreases for R407C, R404A, R507A, and R125 refrigerants, respectively. Augmenting the temperature of the exhaust fluid from the geothermal source increases the exergy efficiency of the cycle for all the refrigerants but has the most significant effect on R125 coolant, after which, R134A, R404A, and R507A refrigerants have a greater effect with the temperature of the exhaust fluid from the geothermal source, while R407C has the slightest changes.

According to Fig. 12, the exergy efficiency augments with isentropic efficiency of compressor for various refrigerants. R134A refrigerant has the highest exergy efficiency, and, then, the exergy efficiency decreases for R407C, R404A, R507A, and R125 refrigerants, respectively. Exergy efficiency changes with the isentropic efficiency of compressor for different refrigerants such as COP with the isentropic efficiency of the compressor.

For the heating process, the significant thermodynamics properties data and exergy rates for geothermal heat pump with R125, R134A, R404A, R407C, and R507A refrigerants are presented in Table 6.

For the heating process, exergy destruction for geothermal heat pump equipment with R125, R134A, R404A, R407C, and R507A refrigerants, presented in Table 7(a–e), is used for the exergy analysis.

The percentage of exergy destruction due to the compressor relative to the exergy destruction due to the overall system for each refrigerant is given in Table 8.

Conclusions

In this investigation, the energy and exergy analysis of a geothermal heat pump cycle and determination of the desired mass flow rate for the cycle are investigated. Also, the optimization of the heat pump cycle is calculated through two methods of maximizing COP and exergy efficiency. The primary outcomes are as follows:

- In the whole system, the maximum exergy loss ratio and the minimum exergy efficiency are observed, respectively, for the compressor and the underground heat exchanger. The exergy loss ratio variations for the compressor with different refrigerants are between 0.26 and 0.29. The exergy efficiency for the underground heat exchanger is also equal to 68.1%. Thus, the compressor and the underground heat exchanger should be improved in the first place.
- The results revealed that, by comparing the mentioned refrigerants for the heat pump cycle, it is observed that R134A and R125 refrigerants have the highest and lowest COP and exergy efficiency, respectively. The COP of the heat pump cycle investigated at the outlet temperature of the geothermal source of 278 (K) with R134A and R125 refrigerants are equal to 4.515 and 4.181, respectively. Under the mentioned condition, the exergy efficiency for R134A and R125 are equal to 0.359 and 0.337, respectively.
- In this cycle, enhancing the temperature of the exhaust fluid from the geothermal source increases the coefficient of operation and exergy efficiency of the cycle. For example, using the R134A refrigerant and variations of outlet temperature of the geothermal source from 278 (K) to 285 (K), the COP of the heat pump cycle increased from 4.515 to 4.525, and the exergy efficiency has risen from 0.359 to 0.36. This means that at a total heating capacity of about 5.6 kW, the increase in heat generation is about 0.11 kW.

The outcomes obtained in present research may provide guidelines for the design and optimization of efficient geothermal heat pump systems, along with some related works like Refs. [49, 50].

References

1. Deymi-Dashtebayaz M, Farahnak M, Moraffa M, Ghalami A, Mohammadi N. Experimental evaluation of refrigerant mass charge and ambient air temperature effects on performance of air-conditioning systems. Heat Mass Transf. 2018;54(3):803–12.
2. Abbasi M, Deymi-Dashtebayaz M, Farzaneh-Gord M, Abbasi S. Assessment of a CHP system based on economical, fuel consumption and environmental considerations. Int J Glob Warm. 2015;7(2):256–69.
3. Chua KJ, Chou SK, Yang WM. Advances in heat pump systems: a review. Appl Energy. 2010;87:3611–24.
4. Ammar Y, Li H, Walsh C, Thornley P, Sharifi V, Roskilly AP. Desalination using low grade heat in the process industry: challenges and perspectives. Appl Therm Eng. 2012;48:446–57.
5. Han X, Chen J, Huang C, Weng W, Wang L, Niu R. Energy audit and air-conditioning system renovation analysis on office buildings using air-source heat pump in Shanghai. Build Serv Eng Res Technol. 2014;35(4):376–92.
6. Tuan CI, Yeh YL, Hsu LF, Chen TC. The pinch technology combined with a heat pump applied in a three-effect evaporator and energy-saving performance assessment. Korean J Chem Eng. 2012;29(3):341–8.
7. Kapustenko PO, Ulyev LM, Boldyryev SA, Garev AO. Integration of a heat pump into the heat supply system of a cheese production plant. Energy. 2008;33(6):882–9.
8. Wu X, Xing Z, He Z, Wang X, Chen W. Performance evaluation of a capacity-regulated high temperature heat pump for waste heat recovery in dyeing industry. Appl Therm Eng. 2016;93:1193–201.
9. Van de Bor DM, Ferreira CI, Kiss AA. Low grade waste heat recovery using heat pumps and power cycles. Energy. 2015;89:864–73.
10. Zhao Z, Xing Z, Hou F, Tian Y, Jiang S. Theoretical and experimental investigation of a novel high temperature heat pump system for recovering heat from refrigeration system. Appl Therm Eng. 2016;107:758–67.
11. Ooka R, Nam Y, Shiba Y, Tanifuji K, Okumura T, Miwa Y. Development of groundwater circulation heat pump system. HVAC&R Res. 2011;17(4):556–65.
12. Lee CK, Lam HN. Determination of groundwater flow direction in thermal response test analysis for geothermal heat pump systems. HVAC&R Res. 2011;17(6):991–9.
13. Aljundi IH. Effect of dry hydrocarbons and critical point temperature on the efficiencies of organic Rankine cycle. Renew Energy. 2011;36(4):1196–202.
14. Tao G, Huaixin W, Liu QL. Measured performances of three working fluids in moderately high-temperature heat pumps. Kung Cheng Je Wu Li Hsueh Pao. 2009;30(10):1628–30.
15. Zhang S, Wang H, Guo T. Experimental investigation of moderately high temperature water source heat pump with non-azeotropic refrigerant mixtures. Appl Energy. 2010;87(5):1554–61.
16. Wang XD, Zhao L, Gao P. Theoretical and experimental analysis of a new zeotropic mixture for moderate and high temperature heat pumps. Kung Cheng Je Wu Li Hsueh Pao. 2008;29(7):1095–8.
17. Nanxi L, Shi L, Lizhong H, Mingshan Z. Moderately high temperature water source heat-pumps using a near-azeotropic refrigerant mixture. Appl Energy. 2005;80(4):435–47.
18. Wang RZ, Li Y. Perspectives for natural working fluids in China. Int J Refrig. 2007;30(4):568–81.
19. Jiang YT, Ma YT, Li MX. Study of two-rotor rolling piston expander used in trans-critical CO_2 compression cycle. Jixie Gongcheng Xuebao. 2010;46(6):139–43.

20. Hou S, Zhang H. An open reversed Brayton cycle with regeneration using moist air for deep freeze cooled by circulating water. Int J Therm Sci. 2009;48(1):218–23.

21. Hou S, Li H, Zhang H. An open air–vapor compression refrigeration system for air-conditioning and desalination on ship. Desalination. 2008;222(1–3):646–55.

22. Hou S, Li H, Zhang H. Open air–vapor compression refrigeration system for air conditioning and hot water cooled by cool water. Energy Convers Manag. 2007;48(8):2255–60.

23. Dincer I. Refrigeration systems and applications. Wiley; 2017.

24. Devotta S, Waghmare AV, Sawant NN, Domkundwar BM. Alternatives to HCFC-22 for air conditioners. Appl Therm Eng. 2001;21(6):703–15.

25. Spatz MW, Motta SFY. An evaluation of options for replacing HCFC-22 in medium temperature refrigeration systems. Int J Refrig. 2004;27(5):475–83.

26. Devotta S, Padalkar AS, Sane NK. Performance assessment of HC-290 as a drop-in substitute to HCFC-22 in a window air conditioner. Int J Refrig. 2005;28(4):594–604.

27. Park KJ, Shim YB, Jung D. Performance of R433A for replacing HCFC22 used in residential air-conditioners and heat pumps. Appl Energy. 2008;85(9):896–900.

28. Park KJ, Jung D. Performance of R290 and R1270 for R22 applications with evaporator and condenser temperature variation. J Mech Sci Technol. 2008;22(3):532–7.

29. Park KJ, Jung D. Performance of heat pumps charged with R170/R290 mixture. Appl Energy. 2009;86(12):2598–603.

30. Park KJ, Shim YB, Jung D. Experimental performance of R432A to replace R22 in residential air-conditioners and heat pumps. Appl Therm Eng. 2009;29(2–3):597–600.

31. Park KJ, Shim YB, Jung D. A 'drop-in'refrigerant R431A for replacing HCFC22 in residential air-conditioners and heat pumps. Energy Convers Manag. 2009;50(7):1671–5.

32. Rosen MA. Does industry embrace exergy. Exergy Int J. 2002;2(4):221–3.

33. Padmanabhan VMV, Palanisamy SK. Exergy efficiency and irreversibility comparison of R22, R134a, R290 and R407C to replace R22 in an air conditioning system. J Mech Sci Technol. 2013;27(3):917–26.

34. Hakkaki-Fard A, Aidoun Z, Ouzzane M. Improving cold climate air-source heat pump performance with refrigerant mixtures. Appl Therm Eng. 2015;78:695–703.

35. Wang XD, Hwang Y, Radermacher R. Two-stage heat pump system with vaporinjected scroll compressor using R410A as a refrigerant. Int J Refrig. 2009;2009(32):1442–51.

36. Baek C, Heo J, Jung J, Cho H, Kim Y. Performance characteristics of two-stage CO_2 heat pump water heater adopting a sub-cooler vapor injection cycle at various operating conditions. Energy. 2014;77:570–8.

37. Rad EA, Maddah S. Entropic optimization of the economizer's pressure in a heat pump cycle integrated with a flash-tank and vapor-injection system. Int J Refrig. 2019;97:56–66.

38. Chao S, Yiqiang J, Yang Y, Shiming D, Xinlei W. A field study of a wastewater source heat pump for domestic hot water heating. Build Serv Eng Res Technol. 2013;34(4):433–48.

39. Huang MJ, Hewitt NJ. The experimental analysis of the effect of ambient factors on the defrosting of economised vapour injection compressor air source heat pump in marine climates. Int J Refrig. 2013;36:820–7.

40. Park C, Lee H, Hwang Y, Radermacher R. Recent advances in vapor compression cycle technologies. Int J Refrig. 2015;60:118–34.

41. Deymi-Dashtebayaz M, Maddah S, Fallahi E. Thermo-economic-environmental optimization of injection mass flow rate in the two-stage compression refrigeration cycle (Case study: Mobarakeh Steel Company in Isfahan, Iran). Int J Refrig. 2019;106:7–17.

42. Rad EA, Maddah S, Mohammadi S. Designing and optimizing a novel cogeneration system for an office building based on thermo-economic and environmental analyses. Renew Energy. 2019. https://doi.org/10.1016/j.renene.2019.11.024.

43. Bertsch SS, Groll EA. Two-stage air-source heat pump for residential heating and cooling applications in northern US climates. Int J Refrig. 2008;31(7):1282–92.

44. Wang W, Ma Z, Jiang Y, Yang Y, Xu S, Yang Z. Field test investigation of a double-stage coupled heat pumps heating system for cold regions. Int J Refrig. 2005;28(5):672–9.

45. Ma GY, Zhao HX. Experimental study of a heat pump system with flash-tank coupled with scroll compressor. Energy Build. 2008;40(5):697–701.

46. Chua KJ, Chou SK. A modular approach to study the performance of a two-stage heat pump system for drying. Appl Therm Eng. 2005;25(8–9):1363–79.

47. Yang D, Song Y, Cao F, Jin L, Wang X. Theoretical and experimental investigation of a combined R134a and transcritical CO_2 heat pump for space heating. Int J Refrig. 2016;72:156–70.

48. Akbulut U, Utlu Z, Kincay O. Exergy, exergoenvironmental and exergoeconomic evaluation of a heat pump-integrated wall heating system. Energy. 2016;107:502–22.

49. Dadsetani R, Sheikhzadeh GA, Safaei MR, Alnaqi AA, Amiriyoon A. Exergoeconomic optimization of liquefying cycle for noble gas argon. Heat Mass Transf. 2019;55(7):1995–2007.

50. Mehrdad S, Dadsetani R, Amiriyoon A, Leon AS, Reza Safaei M, Goodarzi M. Exergo-economic optimization of organic rankine cycle for saving of thermal energy in a sample power plant by using of strength pareto evolutionary algorithm II. Processes. 2020;8(3):264.